
Description of hake (*Merluccius merluccius*) spermatozoa: flagellar wave characteristics and motility parameters in various situations

J. Cosson^{1,*}, A.-L. Groison^{2,3}, C. Fauvel⁴, M. Suquet⁵

¹ UMR 7009, CNRS, Université P. and M. Curie, Cedex, France and Faculty of Fisheries and Protection of Waters, South Bohemian Research Center of Aquaculture and Biodiversity of Hydrocenoses, University of South Bohemia in Ceske Budejovice, Vodnany, Czech Republic

² Department of Biology, University of Bergen

³ Institute of Marine Research, Bergen, Norway

⁴ Ifremer, Station Expérimentale d'Aquaculture, Palavas les Flots

⁵ Ifremer, PFOM/ARN, Argenton, France

*: Corresponding author : J. Cosson, email address : cosson@obs-vlfr.fr

Abstract:

The objective of this study was to complement published hake (*Merluccius merluccius*) sperm motility characteristics by obtention of data more specifically dependent on flagella: beat frequency, flagellar wave amplitude, wave length, number of waves along the length of the flagellum and curvature of the wave. The changes of these parameters are described in relation to the time period elapsed since activation are described using high resolution video images of flagella while quantifying the progression during the swimming period from the activity initiation to full cessation of movement several minutes later. The main characteristic of the swimming period of hake spermatozoa shows a progressive decrease of forward displacement resulting from a cumulative decrease of several activity descriptors: the beat frequency, the percentage of motile cells, the wave amplitude, the number of flagellar waves and the linearity and shape of flagella. All these parameters decrease within 7–8 min after activation in a converging fashion, which leads to full immotility. Measurements of motility parameters at different temperatures also bring additional information about energetic needs for motility of hake sperm. The wave shape of the flagella showed that: (i) the contact of flagella with sea water, not only triggers immediately its motility, but also provokes rapidly local osmotic damages such as blebs which partly impair the correct wave propagation from head vicinity to flagellar tip; (ii) fully developed waves become more and more restricted to the proximal flagellum while the tip becomes devoid of any wave; (iii) the wave amplitude decreases as a function of time during the motility period. The combination of these factors contributes to motility limitations (<100 s) during which the spermatozoa are efficiently able to reach the egg for fertilization. Temperature effects (5–32°C) on these performance characteristics were also studied; this allows to conclude that the amount of energy needed to sustain motility becomes rapidly limiting. A quantitative evaluation of all these sperm motility features leads to a better definition of the conditions for controlled propagation of this species. The motility parameters are also useful as quantitative descriptors of sperm swimming ability in situations such as: (i) varying salinity (osmolality) of the medium (swimming solution) and (ii) activating motility in seminal fluid at various dilution ratios in sea water. All together, our results lead to a better understanding of hake sperm biological features, including its sperm flagella behaviour.

1. Introduction

Comparatively to the recent acquisition of knowledge on sperm behaviour in an increasing number of fish species, very little is known about activation conditions and motility characteristics of spermatozoon of hake, a species of large fishery and/or aquaculture interests. Optimal conditions for flagellar activation, as well as those preventing this activation were defined in the accompanying paper. As in the majority of marine fish species (Cosson et al., 2008 a & b), sperm motility is triggered by the changes in hake spermatozoa microenvironment (osmotic pressure increase) and the motility period is limited to several minutes range, while the efficient progressive period is even more limited as the high velocity (above 50 $\mu\text{m/s}$) period is restricted to about 100 sec. (Groison et al., 2007).

By use of high resolution video microscopy combined with stroboscopic illumination (Cosson et al, 1997; Cosson, 2008) various parameters describing the flagellar behavior during the motility period were investigated, including the measurement of the fraction (MOT%) of active spermatozoa, the flagellar beat frequency, the linearity of the sperm tracks. Details on flagellar shape, waves length and amplitude were obtained as a function of time elapsed in the motility period after sea water triggering and in addition, measurement of flagellar beat frequency at different temperature allows better understanding of energetic constraints involved for movement of hake spermatozoa.

2. Material and Methods

Collection of samples: Sperm samples were collected by stripping wild hakes. Hake perm was collected from 23 ripe males (mean weight \pm SD: 445.2 \pm 262.8g) caught during winter in the Bay of Biscay (France). For technical reasons of samples collection and transportation, the sperm features were assessed after a 48h storage at 4°C.

Sperm preparation and activation: Motility of hake spermatozoa was observed after a first dilution of semen in a diluent at 4°C (see results) followed by a second dilution in sea water directly on the glass slide for observation either at room temperature (22°C) or in some instances after adjustment of temperature by transfer of all the equipment in a thermostated room. Due to the mixing period, first images of swimming spermatozoa could be obtained only after a delay of 5 to 8 seconds.

Microscopic observations : records were mostly as detailed in Cosson et al. (1997) ; phase contrast optics (100X, Zeiss) and dark field video microscopy (Olympus equipped with 40X objective and immersion oil dark field condensor) combined with stroboscopic illumination were used to record spermatozoa at high resolution right after their activation by sea water (SW) and during the whole period of motility, lasting several minutes. Video images were obtained by use of a sVHS video camera (Panasonic, WV AD36-E) and were recorded either on a s-VHS tape recorder (Panasonic, AG 7330) or after digitalisation (using a Formac digital signal transformer) by transfer on a MacBook Pro hard disc for further processing (Cosson et al., 1997). By use of a Hamamatsu DVS-3000 video processor, successive video images were cumulated and used for measurement of the distance covered during a defined period of time (usually one second) which allows to evaluates individual velocity of head traces, as well as the estimation of the percentage of motile cells or that of the linearity of head tracks (Cosson et al., 1997; 2008). Higher magnification images were used to analyze in details the flagellar pattern of individual spermatozoa in terms of wave amplitude, wave length or curvature and their modifications as a function of time after activation. Stroboscopic illumination was used to measure the variation of the beat frequency in Hertz (Hz) during the swimming period by adjustment of light frequency in synchrony with intrinsic beating of individual flagella (Cosson, 2008; Cosson et al., 1997; 2008a).

3. Results

The size of hake spermatozoa cells was measured on video frames recorded from high magnification optical microscopy using either phase contrast or dark field optics. The flagellar length is $47 \mu\text{m} \pm 3 \mu\text{m}$ from dark field images (28 determinations) and $44 \pm 3 \mu\text{m}$ from phase contrast images (23 determinations); some sperm cells presenting loops of flagellar tips (see figure 1) which obviously restricted the flagellar length were rejected in these estimations but constitute precious indicators of the sperm membrane integrity. The head and mitochondria diameter were measured only using phase contrast images and were of $3.1 \pm 0.5 \mu\text{m}$ and $1.3 \pm 0.2 \mu\text{m}$ respectively.

4. General description of the motility period

In all situation described below, motility was observed in media containing an « anti-sticking » compound, (BSA in this case at 1 mg/ml), a condition absolutely necessary to appreciate the actual motility parameters, because it prevents sticking of sperm cells to glass surfaces (Cosson et al., 2003). This allowed to observe that sperm flagella developed planar waves and that, after a short period after mixing sperm in SW, most spermatozoa were swimming in the vicinity of surfaces (glass slide, coverslip or interface between water and air) and sperm cells were very scarce at some distance from surfaces. These conditions allowed to obtain sharp images of flagella recorded at high resolution while swimming (figs. 1 a & b). Before entering more detailed analysis of flagellar characteristics, we present first a general description of the motility period. The duration of the motility period, as estimated as the time period elapsed from activation by transfer in SW to the full arrest of progressive motility which was ranging 2.5 to 3 min.. The efficient forward motility first occurring lasted about 1 min., according to velocity measurements, as detailed further. The percentage of motile spermatozoa vs time slightly declined during a first period, with flagella developing large amplitude waves (fig. 1 a & b). Then during a second period, the percentage of active cells was decreasing more rapidly, and cells which were still active presented flagella with lower wave amplitude (figs. 1 a & b). After this second period (around 2 min. p. a.), a large proportion of spermatozoa were inactive : those remaining active were presenting waves with low amplitude and only located in the proximal part of flagella. In addition, the general shape of active flagella was presenting a bent shape (fig. 1), which is related to more circular tracks described by spermatozoa, as described further in the results. Then spermatozoa entered a period (> 3 min. p. a.) where forward motility ceased : only locally moving spermatozoa were observed with unefficient agitation of flagella (fig 1 a & b).

The resulting ability to forwardly progressing movement during these successive periods is reflected by the velocity parameters vs time. The initial high forward velocity declines after 1 min p. a., and is followed by a period where velocity values are much lower.

From the velocity data collected from swimming assays in SW and in SW/2., it is possible to obtain an evaluation of the total average distance covered by a sperm cell, using the method proposed by Cosson et al. (2008a), which in hake spermatozoa leads to values ranging 3400 to 6600 μm depending on the velocity values considered for calculation (VSL or VAP, see Groison et al., this issue).

Motility of hake spermatozoa in various swimming media

Hake spermatozoa show efficient swimming ability in SW (sea water) and SW/2 as well, (Groison et al., this issue) but sperm motility lasts for longer in SW/2 probably because initial velocity is lower compared to SW. In contrast, spermatozoa cannot swim in SW/4. Motility was evaluated at various salinities/osmolalities in media composed of various ratio of SW in DW. Figure 2 shows results in a graph of % motile cells vs osmolality obtained from the ratio

of SW/SW+DW (diluted SW). From the results observed on three different samples, it is clear that optimal activation occurs for a maximal proportion of cells at salinity above 70% that of SW, with a decline below this value.

Thus, in hake spermatozoa, it appears that the control of motility results from salinity of the surrounding medium. Nevertheless, we observed that sperm swimming occurs in non saline solutions such as 1 M sucrose solution, devoid of any salt and with osmolality ranging that of SW. As discussed later, in hake like in most fish species so far studied (Cosson et al., 2008a), motility appears to be mostly controlled by osmolality external to the cell.

In undiluted seminal fluid (SF), few spermatozoa do swim but for very brief and transient periods after dilution in SF. When SF was partly diluted by SW, a higher proportion of spermatozoa is activated : in figure 3, various dilutions of SF by SW were assayed and plotted as the % motile cells vs dilution of SF (ratio SF/SF+SW) on three different samples. A sharp increase of motility is observed when SF is weakly diluted by SW (1 volume of SW combined with 3 volumes of SF or above). Therefore, it is proposed that motility of hake spermatozoa is controlled by osmolality of the SF, but the osmolality value was not directly measured in these experiments.

During the motility phase, a very initial period is observed during which tracks are almost linear with little lateral head deviation (fig. 4). Circling of sperm tracks appears later in the motility period in the form of large circles initially and followed subsequently by tighter circles becoming very tight at the end of movement period. Figure 4 shows sperm tracks (1 sec. each) at 6 successive time periods as indicated (see bottom right in each panel).

As briefly mentioned, most spermatozoa swim at glass/water or water/air interfaces (Cosson et al., 2003): a brief estimation leads to values of 49% swimming at top and 49% at bottom, at 15 sec (or later) after activation. At the end of the motility period, the same estimation leads to values higher than 49% at bottom (interface glassslide/water) which has been called « sinking artifact » (Cosson et al., 2003). Most important, it is worth to remark that circling is counter clockwise when observed from top of drop at the interface air/water and clockwise at interface water/glass slide, as observed for spermatozoa of other species (Cosson et al., 2003).

5. The wave shape of flagella is changing in several respects during the motility period

The full waves pattern appears initially right after activation (fig. 1a, left pannel) but gradually during the motility period, only proximal waves remain present along flagella (Fig 1a, middle pannels). In figure 1b are shown successive positions of flagellar waves as observed in series of video frames obtained every 50th of second and corresponding to several time periods along the motility phase.

The successive patterns exhibited by the flagella during the motility period are schematically summarized in the drawing of figure 1c : in 1- the flagellum is straight since it is not activated ; in 2- right after activation in SW, waves are present all along the flagellum which presents a slightly curved envelope (see median line) ; in 3- a decrease of wave amplitude occurs later, while the envelope curvature increases ; in 4 and 5- waves are still developed but only in the proximal portion and the flagellar envelope becomes very curved.

Measurements of flagellar waves parameters during the motility period

The wave amplitude was measured at various time periods post activation as shown in figure 5a, which shows the mean value of the first wave, closest to the head (see fig. 5b, bottom) as a function of time (3 different sperm samples, mean of 5 evaluations for each point).

The wave amplitude remains quite constant during a first period lasting about 60 sec., then declines gradually towards the end of the motility period. As a complement, the amplitude of

each individual wave (a maximum of 4 waves are covering the whole flagellar length) was measured vs time after activation, as shown in figure 5b (mean of 5 evaluations per each point). It is clear that waves 1 and 2 (see definition at bottom of fig. 5b) remain constant with an amplitude around 5 μm for a period up to 30 sec then the amplitude decreases, but more slowly than that of waves 3 and 4 located more distally along the flagellum.

As predictable from figures 1 and 5b, the number of waves traversing the flagellar length is decreasing during the motility period : this point is illustrated in figure 5c which shows a decline of the number of curvatures observed along flagella during the sperm motility period. Obviously, such decline also participates to the general decrease of swimming efficiency of hake spermatozoa during its progression in the motility period.

The evolution of the flagellar beat frequency during the motility period: The flagellar beat frequency (FBF) was measured at various time points post activation and figure 6 shows the evolution of the FBF vs time plotted for 3 different sperm samples. In this graph, the FBF values only account for moving cells and do not include immotile cells (obviously with FBF = 0).

When the FBF was measured at different temperatures, the FBF values were decreasing while temperature was decreased : figure 7a shows a graph of BF vs temperature.

These data can be presented as in the graph of figure 7b where $\ln \text{FBF}/T$ is plotted vs $1/T$, where T is the absolute temperature (degrees Kelvin) ; this representation, also known as « Arrhenius plot », allows to get access to the value of two important parameters, the free energy (ΔH) and enthalpy (ΔS) of the ATP hydrolysis reaction (Holwill and Silvester, 1967) which controls the BF of sperm flagella (Gibbons, 1981). Measurements of ΔH and ΔS can be deduced from this graph as detailed below in the discussion paragraph, by measuring the slope and the intercept with x axis, leading to values of 10.945 Kcal.mol⁻¹ and 13.735 e.u. (entropy units) respectively.

6. Discussion

The description of the salient features occurring during the motility period of hake spermatozoa can be envisioned according to two complementary approaches : either using parameters describing the flagella movements or by measurements of the head displacement features ; it is obvious that the two sets of data are highly linked as head movements reflect directly those of flagella, both organelles being held by the same cell, the spermatozoon. In the case of hake spermatozoa, head movement characteristics were described in the accompanying paper (Groison et al., this issue) while the main flagellar parameters were acquired from additional data described in the present paper (table 1) and one aim of the latter is also to establish the relationships with the former.

Activation of hake spermatozoa occurs right at contact with SW but also with lower salinity media (SW/2) as shown in figure 2, where SW was diluted in various ratio by DW. In these experiments, salinity reflects osmolality effects of the surrounding medium as non ionic solutions of 1M sucrose with osmolality similar to that SW provokes similar activation of motility. The osmotic control of motility occurs similarly when spermatozoa are transferred in diluted SF : a low dilution of SF by SW is enough to trigger motility as shown in figure 3. It is worth to mention that motility activation is fully reversible : when sperm firstly activated in SW for few seconds its motility immediately stops following a subsequent transfer in 4X diluted SW (data not shown). Therefore, hake spermatozoa are in conformity with many fish species studied so far: activation of sperm motility occurs through an osmotic signal (Morisawa, 1985 ; 1994; Cosson et al., 2008b) generated by a gradient of osmolality between the inside and outside of the sperm cell. In marine fish spermatozoa, this osmolar membrane signal would be transduced to the flagellar motor apparatus via an intracellular ionic relay (Cosson et al. 2008b).

Right after transfer into SW, activation occurs immediately and is followed by a motility period lasting about 2-3 min in SW but for longer in diluted SW (up to 15 min in SW/2) as was already emphasized in the accompanying paper (Groison et al., this issue). Whatever the osmolality of the swimming solution (either ranging from around 1100 mOsmol.Kg⁻¹ in SW or ranging 550 mOsmol.Kg⁻¹ in SW/2) all motility parameters decline during the motility period (Groison et al., this issue) which reflects consequently a parallel decline of the flagellar movement parameters described in details in the present paper. Such decline feature is also shared with spermatozoa of many other fish species (Cosson et al., 2008 a & b) and is also partly due to blebs appearing at the flagellar tips, probably resulting to curling engendered by the osmotic shock received by the sperm cells at transfer into SW (fig. 1). In some spermatozoa, the tip curling restricts the flagellar length in such a way that the efficient distance along which flagella develop waves is 1/4th to 1/3rd shorter for part of the sperm cells population : such curling appears more and more frequently as the swimming period progresses.

Among the flagellar parameters, some have more crucial roles than others in their participation to the global displacement efficiency, usually reflected in the forward velocity of translation. Below are considered successively : the amplitude and length of each flagellar wave, the curvature of the wave pattern and the flagellar beat frequency.

Regarding the wave amplitude (fig. 5a & b), its value remains quite stable during the first period (60 sec.) following activation, then gradually decreases to lower value leading to poorer efficiency for propelling sperm cells. In contrast, the wave length is little affected and its value ranges 12 µm during most of the motility period (data not detailed). The decrease in the number of waves (or curvatures) along the flagellum (see figure 5c) also participates to the fall down process of the propulsive efficiency during the motility period. The distal part of the flagellum thus becomes devoid of waves, a feature which could be in relation with the decrease of intracellular ATP when reaching the end of the motility period. This feature is also present in turbot (Perchee et al., 1993) or trout (Saudrais et al., 1998) spermatozoa and was hypothetically associated with a lack of distribution of ATP molecules originating from mitochondria where sperm ATP is produced : mitochondria being located in the vicinity of the sperm head, a shuttle distributing ATP molecules all along the flagellum and using creatine phosphate and creatine kinase (Saudrais et al., 1998) would be necessary but should operate fast enough to sustain an homogeneous distribution of ATP all along the flagellum, which is not the case in fish sperm flagella.

The curvature of the beating envelope (defined as the area in which the flagellum develops its waves) is gradually increasing during the motility period (see fig. 1, especially 1c) which leads directly to the circularization of the swimming tracks followed by sperm cells (see fig. 4). Such change in the diameter of the swimming tracks has been related, in other species such as sea urchin, trout, sea bass or tuna (Brokaw, 1991 ; Boitano and Omoto, 1992 ; Cosson et al, 1989 ; Dreanno et al., 1999 ; Cosson et al., 2008a) to the involvement of the Ca²⁺ ions. When the intracellular Ca²⁺ ions concentration increases, the beating of flagella becomes more assymetrical (fig. 1) and therefore the circling tracks described by sperm cells become tighter, that is of smaller diameter (see fig. 4). It is obvious that such increase of circling of spermatozoa will decrease the volume for exploring the water space (as cells will move only locally) and impair the probability for egg meeting, but could increase the chance of entering the egg micropyle.

The flagellar beat frequency is an important parameter to be considered : it represents a measurement of the number of beats generated by a flagellum every second and has been shown to be linearly related on theoretical bases (Holwill, 1969) to : 1) the velocity of forward displacement (Denehy, 1975) and 2) the rate of energy consumption (ATP) by the propulsive device present in sperm flagella (Gibbons, 1981). Both aspects are discussed for hake spermatozoa in the following paragraphs in order to evaluate the respective relationships between beat frequency and velocity on one hand and between propulsivity and ATP consumption on the other hand.

As far as point 1) is concerned, a limited number of parameters (waves length and amplitude, beat frequency, head and flagellar size) can be used for elaboration of an hydrodynamic

model of a swimming spermatozoon and the relationship between these parameters has been formalized in the following equation (Gray and Hancock, 1955 ; Denehy, 1975) :

$$V_x = 2f \pi^2 b^2 / \lambda \{ 1/1 + 4\pi^2 b^2 / \lambda^2 - (1 + 2\pi^2 b^2 / \lambda^2)^{1/2} - 3a/n\lambda [(\ln d/2\lambda) + 1] \} \quad \text{eq. 1}$$

where V_x is the velocity of propulsion of the spermatozoon, b is the amplitude of wave, λ is the length of wave, n is the number of simultaneous waves, f is the beat frequency of waves, a is the radius of head and d is the radius of tail. The relationship predicts that the wave amplitude and the beat frequency are two crucial parameters (dependency is to the square of their value) while the wave length is of lower influence (linear dependency). Application of this formula leads to some of the data in table 1, which compares predictions and experimental values of the swimming parameters.

Regarding point 2) the following formula was established by Holwill (1969) and verified for spermatozoa of several flagellated species. It relates the FBF (f) to two energetic parameters, ΔH and ΔS , as they will be defined below:

$$\ln (f/T) = [\Delta S/R / \ln (k/h)] - \Delta H/RT \quad \text{eq. 2}$$

where f is the flagellar beat frequency, T the absolute temperature in °Kelvins, ΔS the change in entropy of the reaction, ΔH the change in enthalpy, R the gas constant, k the Boltzman constant and h the Planck constant. The application of this formula is presented in figure 7 and is discussed later.

Regarding predicted and experimental values of hake spermatozoa velocity, it appears that some agreement is observed (table 1) for results of the present paper, even considering the values at 90 and 180 sec. post activation which correspond to spermatozoa swimming with non optimal performances. The hydrodynamic model sustaining the formula (eq.1) used for predictions is based on optimal performances of an ideal spermatozoon (Gray and Handock, 1955) with waves present all along the flagellum, which is not the case for hake sperm half way in its motility period (see fig.1). Also, table 1 shows some discrepancy between velocity values of the present paper and those obtained in the accompanying paper (Groison et al., this issue). This discrepancy is only apparent : it emphasizes the need for using standardized method when comparing results obtained by different methodologies (Fauvel et al., this issue), the later providing access to subtle ways of describing sperm movement but complicating the comprehensivity of comparisons between various situations.

An additional aim of the present paper is its approach of an important aspect of sperm function, that of power expenditure for sustainement of motility. This power expenditure can be evaluated when measurements of one key motility parameter can be obtained at different temperatures as detailed below. This is probably of importance at egg fertilization when sperm must approach then contact the egg, both steps which must occur at optimal temperature. It is clear that temperature appears as an adverse factor to ability to fertilize as the decrease of temperature leads to reduce BF and therefore translational velocity. Such apparent disadvantages could be compensated by an opposite effect of temperature : decrease of temperature leads to increase the duration of motility (Billard and Cosson, 1988 ; Alavi and Cosson, 2001) and thus increases statistically the chances of meeting between egg and sperm. From a thermodynamic point of view, one must also consider that pressure represents an additional aspect possibly acting on sperm performances, taking account that sperm spawning occurs in deep water in some marine fish species. These principles (energy, temperature and pressure) can be simply summarized and formalized by application of general laws of thermodynamics in which data from our results can be incorporated. One such law allows to relate any chemical reaction to energetic parameters of spermatozoa (Holwill and Silvester, 1967). When applied to hake sperm flagella, such principle can be used to describe the chemical reaction leading to flagellar movement, i. e. beat frequency and thus can be described by the equation :

$$\ln f/T = A + \Delta S/R - \Delta H/RT \quad \text{eq. 3}$$

where f = flagellar beat frequency, T = absolute temperature in °Kelvins, ΔS = change in entropy, ΔH = change in enthalpy, A is a constant such that $A = \ln k/h$ where k is the Boltzmann constant ($k = 1,38 \cdot 10^{-23} \text{ J.K}^{-1} = 0,3296 \cdot 10^{-23} \text{ Cal.K}^{-1}$) and h is the Planck constant ($h = 6,626 \cdot 10^{-34} \text{ J.s} = 1,682 \cdot 10^{-34} \text{ J.s}$).

Knowing that $\Delta H = \Delta E + p\Delta V$, where ΔE is change in energy, one obtains the relation:

$$\ln f/T = A + \Delta S/R - \Delta E/RT - p\Delta V/RT \quad \text{eq. 4}$$

where p is the pressure and ΔV is the change in volume; equation (2) comprises 3 terms corresponding to the three aspects above mentioned: first term is $\Delta S/R$ and relates to entropy, second term is $\Delta E/RT$ and relates to energy while third term is $p\Delta V/RT$ and relates to pressure and volume. In the case of hake, the pressure term can probably be eliminated as it is believed that hake spawning and reproduction occur at depth ranging 100 to 200 m (Alvarez et al., 2001; Olivar et al., 2003). A calculation using the above formula shows that the effect of pressure on motility parameters is low at such pressure and would be influential only for pressure values corresponding to 600 m depth or below.

The temperature at which hake spawning and fertilization occurs is ranging 10°C according to several authors (Alvarez et al., 2001; Olivar et al., 2003). Therefore it would be a better strategy to evaluate the sperm motility parameters at this temperature, but for technical reasons (microscope stage thermostatisation), it is much easier to run motility assays at room temperature, usually 22-24°C. It appears from figure 7b, where $\ln f/T$ is plotted as a function of $(1/T)$, that this plot reflects a linear relationship which allows to get the values of slope and intercept with x axis which are directly related to ΔS and ΔH by the equation (3):

$$\ln f/T = \{\Delta S/R + \ln(k/h)\} - \Delta H/RT \quad (3)$$

when applied to hake sperm (figure 7b), this plot leads actually to a straight line where its intercept with x axis provides the value of $\Delta S = -13.735$ e.u. (entropy units) and from slope leads to a value of $\Delta H = 10.945 \text{ Kcal.mol}^{-1}$. Knowing that $\Delta G = \Delta H - T\Delta S$, one obtains $\Delta G = 6.921 \text{ Kcal.mol}^{-1}$. This value represents the minimal free energy necessary to accomplish the limiting reaction for optimal flagellar movement and which controls the FBF.

From independent thermodynamic data, it is usually estimated that the total amount of free energy delivered by the reaction of hydrolysis of ATP is ranging value of $\Delta G = -31 \text{ KJ.mol}^{-1}$ or $= -7.4 \text{ Kcal.mol}^{-1}$. The ΔG values are worth to compare in case of hake spermatozoa: the energy need for movement corresponds to a ΔG of $6.921 \text{ Kcal.mol}^{-1}$ while the total available energy for movement corresponds to a ΔG of $-7.4 \text{ Kcal.mol}^{-1}$, therefore it appears that most of this available energy (89%) must be devoted to movement, which may severely impair other ATP requesting functions such as membrane ionic pumps, thus probably resulting in an intracellular Ca^{2+} ions accumulation, leading to flagellar asymmetry and resulting in circling of tracks as discussed above. It will be worth in future experiments to relate these results to the actual ATP consumption of hake sperm during the motility period. According to the accompanying paper (Groison et al., this issue), the energetic stores (AEC) and specially the ATP concentration is ranging 200 nanomoles per 10^9 spermatozoa right before entering the motility period. By analogy with spermatozoa of many other fish species (Cosson et al., 2008a), the ATP stores are decreasing during the motility period, a feature which is predictable for hake sperm due to the observed decrease of the flagellar beat frequency. The above calculation leading to optimal consumption of energy holds certainly for a short period right after motility activation, but, due to the rapid exhaustion of the ATP stores, these conditions are reaching values much lower than optimal and therefore, as observed in other species, all motility parameters of hake sperm are observed to decrease, down to an extreme situation at the very end of the motility period where the available ATP is fully lacking and therefore any motility stops. This situation of ATP limitation is even worst in the

distal portion of fish sperm flagella where diffusion of ATP is lacking due to the distance to the ATP source, i. e. mitochondria (Yanagisawa et al., 1968 ; Tombes et al., 1987), which leads to flagellar dampening (fig. 1). Because, in hake spermatozoa, the amount of ATP available for motility is probably limited to the stores amassed before motility triggering, this restrictive limitation results in a possible translating distance covered in average by spermatozoa of 3.4 to 7.7 mm, a range of values which, compared to the egg diameter which ranges 0.93 to 1.17 mm in European hake (Alvarez et al., 2001), emphasizes why reproduction strategy imposes vicinity constraints between male and female spawners.

References

- Alvarez, P.; Motos, L.; Uriarte, A.; Egaña, J., 2001: Spatial and temporal distribution of European hake, *Merluccius merluccius* (L.), eggs and larvae in relation to hydrographical conditions in the Bay of Biscay. Fisheries Research. **50**, 111-128.
- Billard, R.; Cosson, M.-P., 1988: Sperm motility in rainbow trout *Parasalmo mykiss* : effect of pH and temperature. In : *Reproduction in Fish Basic and Applied Aspect in Endocrinology and Genetics* (Breton, B. & Zohar, Y. eds) pp161-167 INRA Paris.
- Boitono, S.; Omoto, C.K., 1992: Trout sperm swimming patterns of role of intracellular Ca^{2+} . Cell Mot. and the Cytoskel. **21**, 74-82.
- Brokaw, C. J., 1991: Calcium sensors in sea urchin sperm flagella. Cell Mot. and the Cytoskel. **18**, 123-130.
- Cosson, J., 2008: Methods to analyse the movements of fish spermatozoa and their flagella. in "*Fish Spermatology*" Alavi, S.M.H.; Cosson, J.J.; Coward, K. and Rafiee, G. Eds, Oxford, Alpha Science International Ltd., pp. 63-101.
- Cosson, J.; Billard, R.; Cibert, C.; Dreanno, C.; Linhart, O.; Suquet, M., 1997: Movements of Fish Sperm Flagella studied by High Speed Videomicroscopy coupled to Computer Assisted Image Analysis. Polish Arch. Hydrobiol. **44** ,103-113.
- Cosson, J., Groison, A. L., Suquet, M., Fauvel, C., Dreanno, C., Billard R., 2008a: Studying sperm motility in marine fish : an overview on the state of the art. J. Appl. Ichthyol. **24**, 460-486.
- Cosson, J.; Dreanno, C. ; Fauvel, C.; Groison, A.-L.; Suquet, M.; Billard, R., 2008b: Marine fish spermatozoa : racing ephemeral swimmers. Reproduction **136**, 277-294.
- Cosson, J., Huitorel, P., Gagnon, C., 2003: How spermatozoa come to be confined to surfaces. Cell Mot. & Cytoskel. **54**, 56-63.
- Cosson, M.P.; Billard, R.; Letellier, L., 1989: Rise on internal Ca^{2+} accompanies the initiation of trout sperm motility. Cell Mot. and the Cytoskel. **14**, 424-434.
- Denehy, M. A., 1975: The propulsion of nonrotating ram and oyster spermatozoa. Biol. Reprod. **13**, 17-29.
- Dreanno, C.; Cosson, J.; Suquet, M.; Dorange, G.; Fauvel, C.; Cibert, C.; Billard, R., 1999: Effects of osmolality, morphology and intracellular nucleotid content during the movement of sea bass (*Dicentrarchus labrax*) spermatozoa. J. Reprod. and Fertil. **116**, 113-125.
- Fauvel, C.; Suquet, M.; Cosson, J., 1999: Evaluation of fish sperm quality. J. Appl. Ichthyol. [this issue](#).
- Gibbons, I. R., 1981: Cilia and flagella of eukaryotes. J. Cell Biol. **91**, 107s-124s.
- Groison, A.-L.; Suquet, M.; Cosson, J.; Le Coz, J.-R.; Jolivet, A.; Garren, F., 2007: Sperm biological characteristics in European hake (*Merluccius merluccius*). Cybium **32(2)**, 178.
- Groison, A.-L.; Fauvel, C.; Suquet, M.; Kjesbu O. S.; Le Coz, J.-R.; Mayer I.; Cosson, J., 2009: Some characteristics of sperm motility in European hake (*Merluccius merluccius*, L., 1758). J. Appl. Ichthyol. [this issue](#).
- Holwill, M. E., 1969: Kinetic studies of the flagellar movement of sea-urchin spermatozoa. J. Exp. Biol. **50**, 203-22.
- Holwill, M.E.; Silvester N. R., 1967: Thermodynamic aspects of flagellar activity. J. Exp Biol. **47**, 249-65.

Morisawa, M., 1985: Initiation mechanism of sperm motility at spawning in teleost. *Zool. Sci.* **2**, 605-615.

Morisawa, M., 1994: Cell signalling mechanism for sperm motility. *Zool. Sci.* **11**, 647-662.

Olivar, M. P.; Quílez, G.; Emelianov, M., 2003: Spatial and temporal distribution and abundance of European hake, *Merluccius merluccius*, eggs and larvae in the Catalan coast (NW Mediterranean), *Fisheries Res.* **60**, 321-331.

Perchec, G.; Chauvaud, L.; Suquet, M.; Cosson, J.; André, F.; Billard, R., 1993: Changes in the movement characteristics and ATP content in the sperm of carp and turbot (teleost fishes) - *C.R. Acad. Agri.* **6**, 117-126.

Tombes, R.M.; Brokaw, C.J.; Shapiro, B.M., 1987: Creatine kinase dependent energy transport in sea urchin spermatozoa. Flagellar wave attenuation and theoretical analysis of high energy phosphate diffusion. *Biophys. J.* **52**, 75-86.

Saudrais, C.; Fierville, F.; Cibert, C.; Loir, M.; Le Rumeur, E.; Cosson J., 1998: The use of creatine-phosphate plus ADP as energy source for motility of membrane deprived trout spermatozoa. *Cell Mot. and the Cytosk.* **41**, 91-106.

Yanagisawa, T.; Hasegawa, S.; Mohri, H. 1968: The bound nucleotides of the isolated microtubules of sea-urchin sperm flagella and their possible role in flagellar movement. *Exp. Cell Res.* **52** 86-100.

Tables

Table 1 : predicted and measured velocity of hake spermatozoa after activation in sea water.

<i>Parameter</i>	At earliest time	At 90 sec	At 180 sec
<i>FBF => f (Hz)</i>	53	29	10
<i>Wave amplitude => b (μm)</i>	4	2.5	0.5
<i>Wave length => λ (μm)</i>	12	10	12
<i>Head radius => a (μm)</i>	1.5	1.5	1.5
<i>Number of waves => n</i>	4	2.6	0.5
<i>Tail radius => d (μm)</i>	0.15	0.15	0.15
Calculated velocity in this paper (μm/sec)	231	86	<10
<i>VAP (μm/sec) (accompanying paper)</i>	64 +/- 23	24 +/- 5	19 +/- 3
<i>VCCL (μm/sec) (accompanying paper)</i>	82 +/- 25	42 +/- 10	40 +/- 5
<i>VSL (μm/sec) (accompanying paper)</i>	51 +/- 22	14 +/- 7	11 +/- 4
<i>% MOT (accompanying paper)</i>	75 +/- 16	34 +/- 18	18 +/- 10
Measured velocity in this paper (μm/sec)	180 - 162	130 - 39	20 - 5
<i>% MOT (this paper)</i>	90	30	25

Legend of table 1: Parameter values used for velocity calculation (f, b, λ, a, n and d as defined in the related to eq. 1) are obtained from results from the present paper. FBF (f) is the flagellar beat frequency. VAP, VCCL, VSL and %MOT represent velocity parameters and fraction of motile spermatozoa as defined in Groison et al. ([this issue](#)).

Legends of the figures :

Legend of fig 1a: Series of video frames of different hake spermatozoa obtained by single flash exposures. The frames from left to right were at 9, 23, 72 and 154 seconds respectively, after motility activation in sea water. Anomalies such as blebs or excrescences are visible punctually on some flagella (see bar scale in fig. 1b).

Legend of fig 1b: The photomontage shows successive images (every 50th of sec) of the same spermatozoon in each series, activated in SW since 17 seconds (upper pannel), 41 sec (lower pannel, left), 77 sec (lower pannel, center) and 139 sec (lower pannel, right) respectively. (Bar scale = 10 μ m between 2 lines).

Legend of figure 1c: This series of drawings explains how two changes of flagellar shape occur during the motility period : 1- before activation, 2- few seconds after activation by SW, large amplitude waves are present all along the flagellum and the wave envelope is only slightly curved, almost linear 3- waves decrease in amplitude specially in the distal portion of flagellum at later period of motility and envelope becomes curved with time ; this curvature explains circularity of tracks becoming tighter and tighter circles shape. Situation (1) is observed before activation, (2) is 5-15 sec after activation in SW, (3) is 30-40 sec after transfer in SW, (4) is after 1 min or so, (5) is later on and (6) is observed at very end of the motility period where all spermatozoa stopped. The mid line indicates the curvature of the flagellar envelope (surface in which the flagellum swims).

Legend of fig. 2: Variation of the percentage of motile hake spermatozoa as a function of the salinity of the swimming solution : sea water (SW) diluted in various ratios by distilled water (DW) was used as swimming medium and after video recording, the percentage of swimming cells was estimated on three different samples.

Legend of fig. 3: Variation of the percentage of motile hake spermatozoa as a function of the dilution ratio of seminal fluid by SW. The seminal fluid was collected by centrifugation at 3000g for 15 min. to eliminate sperm cells and debris. The resulting supernatant was used as swimming medium, either undiluted or after dilution by SW and after addition of a small volume of sperm (see material and methods) the percentage of swimming cells was estimated on three different samples in such diluted SF.

Legend of fig. 4: Variation of the sperm tracks diameter as a function of the advancement in the swimming period. Head tracks were generated by images accumulation of successive video frames during one second. This photo montage shows sperm head tracks at 6 successive time points (from left to right and top to bottom respectively) corresponding to 22, 39, 66, 82, 98 and 136 seconds after activation in SW.

Legend of fig. 5a: Average amplitude of the flagellar waves of hake spermatozoa as a function of the advancement in the motility period. Amplitude was measured on video images similar to those presented in fig. 1, using 3 different samples and 5 different sperm images for each time point.

Legend of fig. 5b: Amplitude of individual flagellar waves of hake spermatozoa as a function of the advancement in the motility period. Amplitude was measured in fig. 5a, but each one of the 4 waves along the flagellum was measured separately, according to the wave position as numbered at bottom left of the graph.

Legend of fig. 5c: Number of curvatures along individual flagella of hake spermatozoa as a function of the advancement in the motility period. Waves were according to the wave position as numbered at bottom left of the graph.

Legend of fig. 6: Variation of the beat frequency of hake sperm flagella as a function of time in the motility period. The FBF was measured by stroboscopy on 10 different sperm cells using 3 different sperm samples at the different time points in the motility period indicated in abscissae of the graph.

Legend of fig. 7a: Variation of the beat frequency of hake sperm flagella as a function of temperature. At each temperature, the FBF was measured by stroboscopy on 10 different

sperm cells for 3 different sperm samples at a time point corresponding to 20-25 seconds in the motility period.

Legend of fig. 7b: Arrhenius plot of beat frequency of hake sperm flagella. Results of fig.7a are plotted as the neperian logarithm of the ratio between the FBF and the absolute temperature (in degrees Kelvin) in ordinate relative to the reverse of absolute temperature in abscissae.

Figures and graphs



Figure 1a

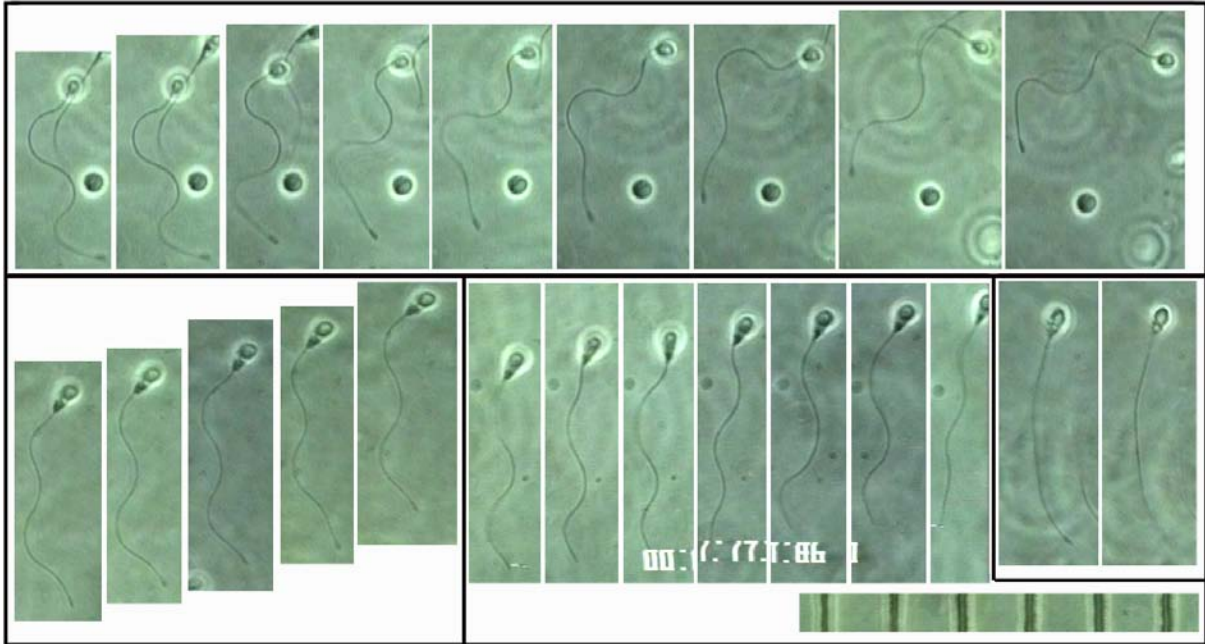


Figure 1b

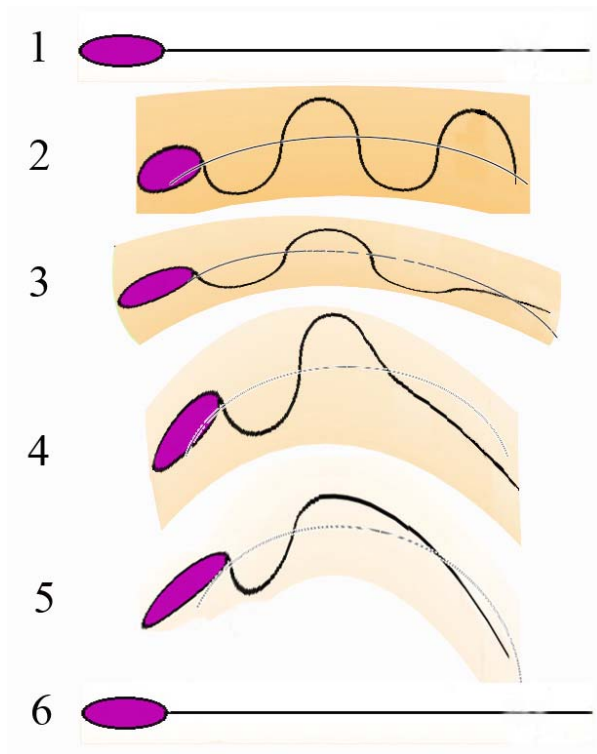


Figure 1c

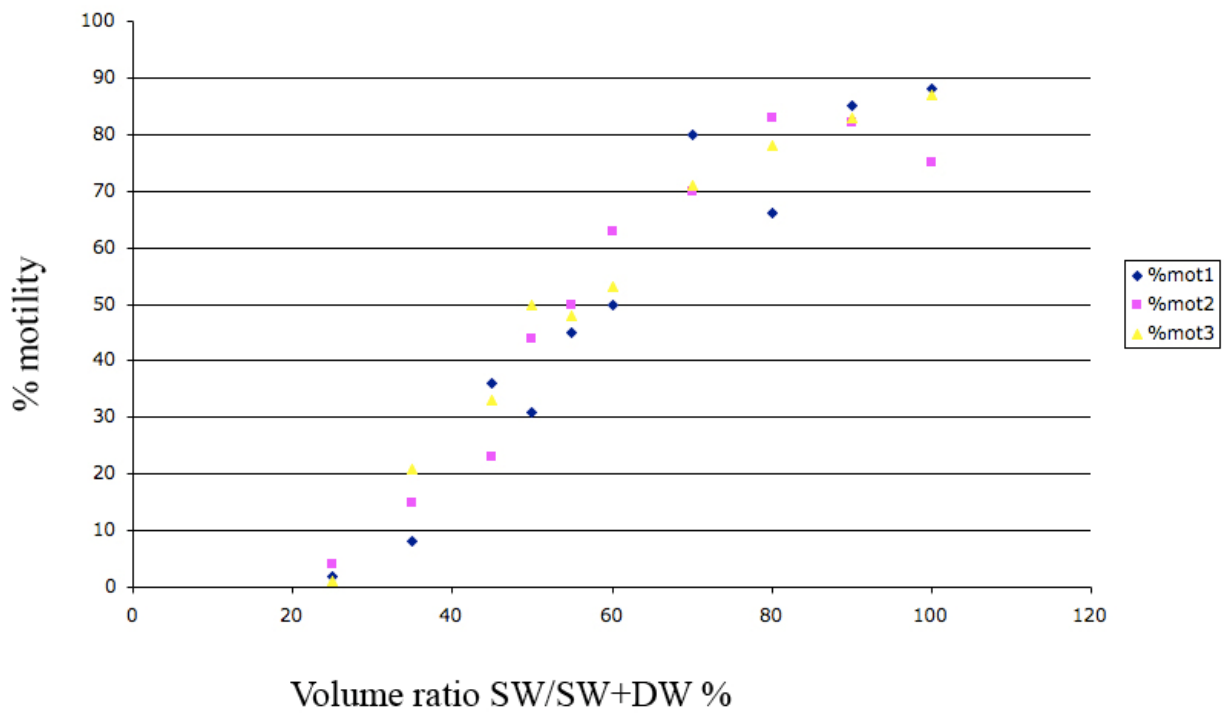


Figure 2

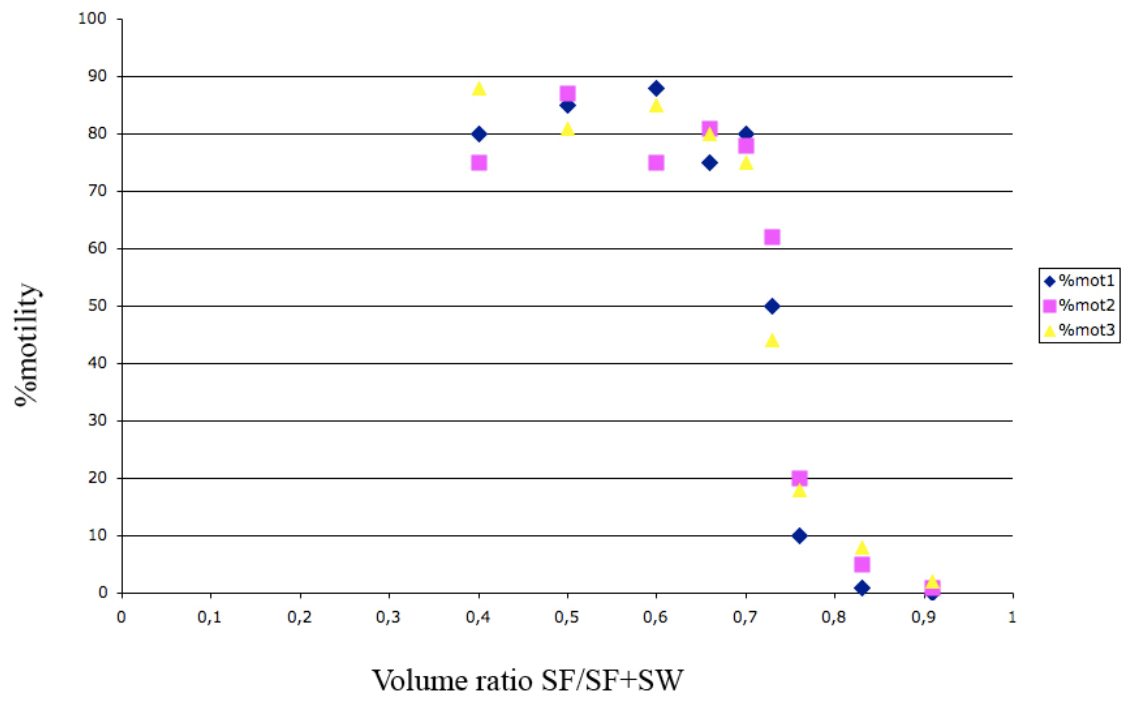


Figure 3

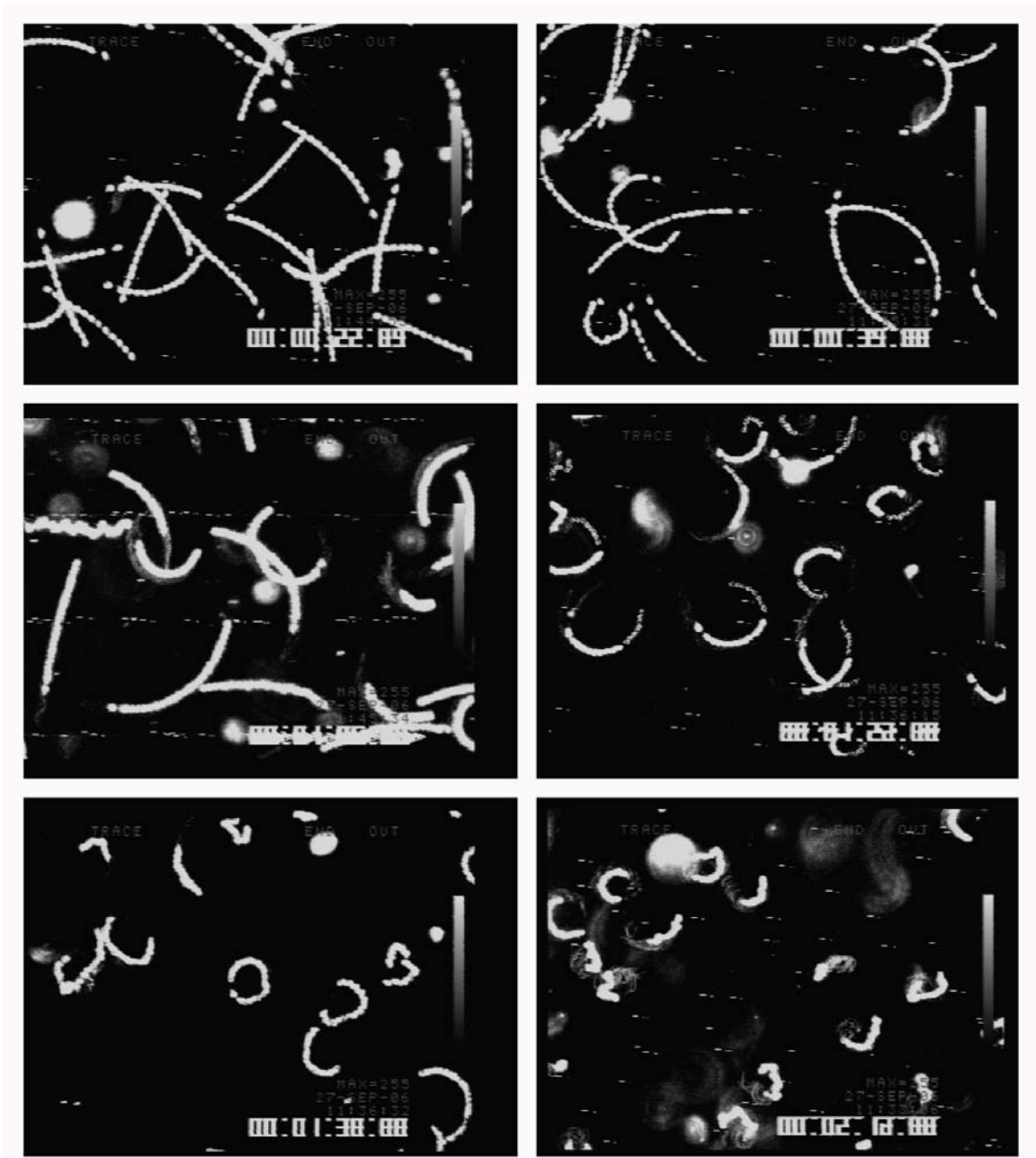


Figure 4

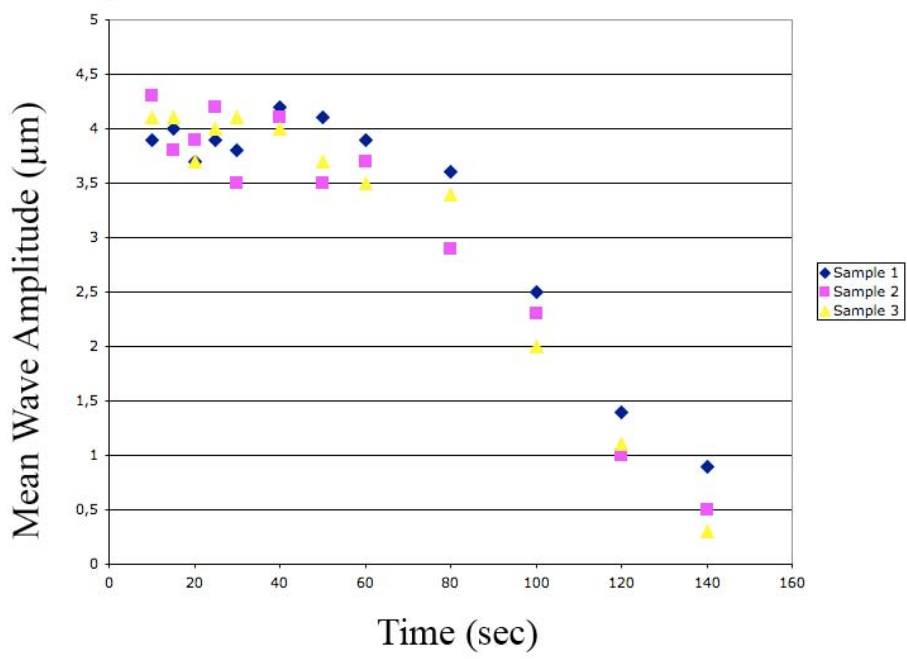


Figure 5a

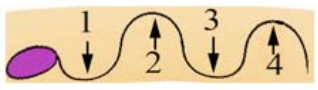
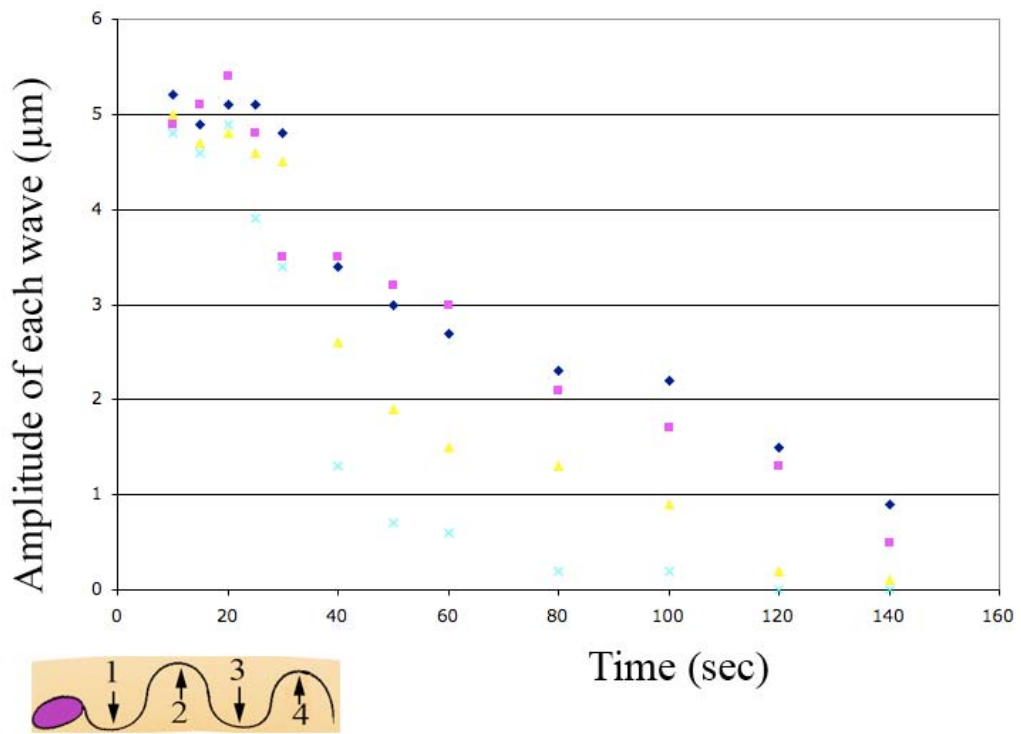


Figure 5b

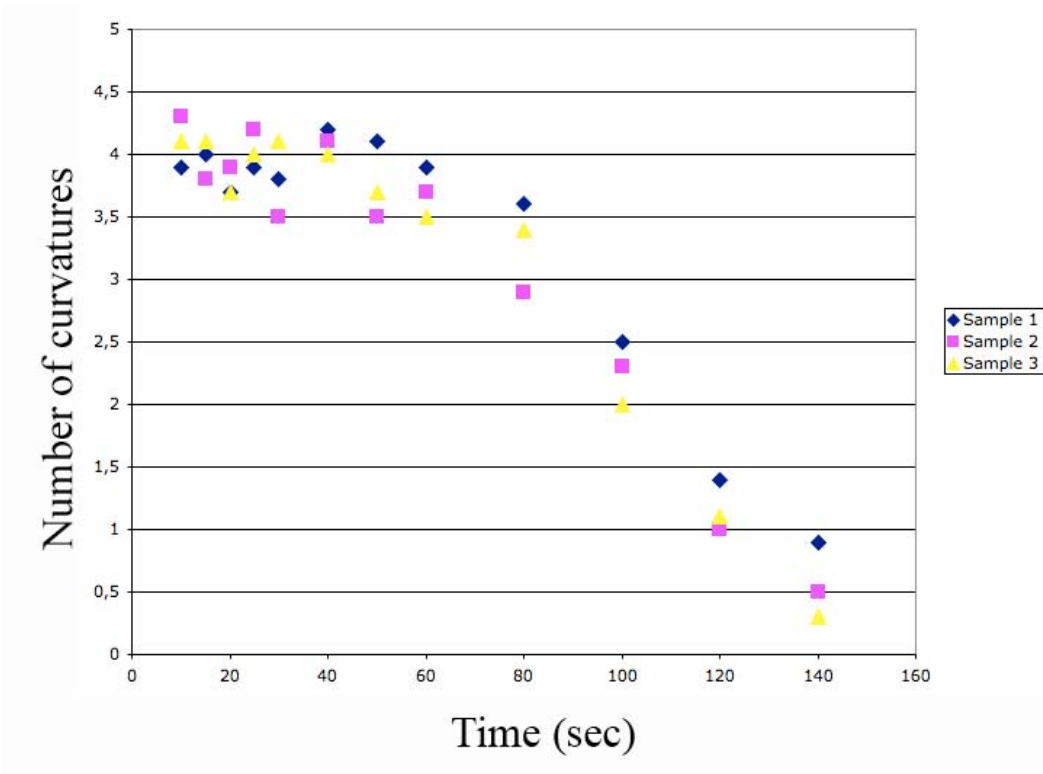


Figure 5c

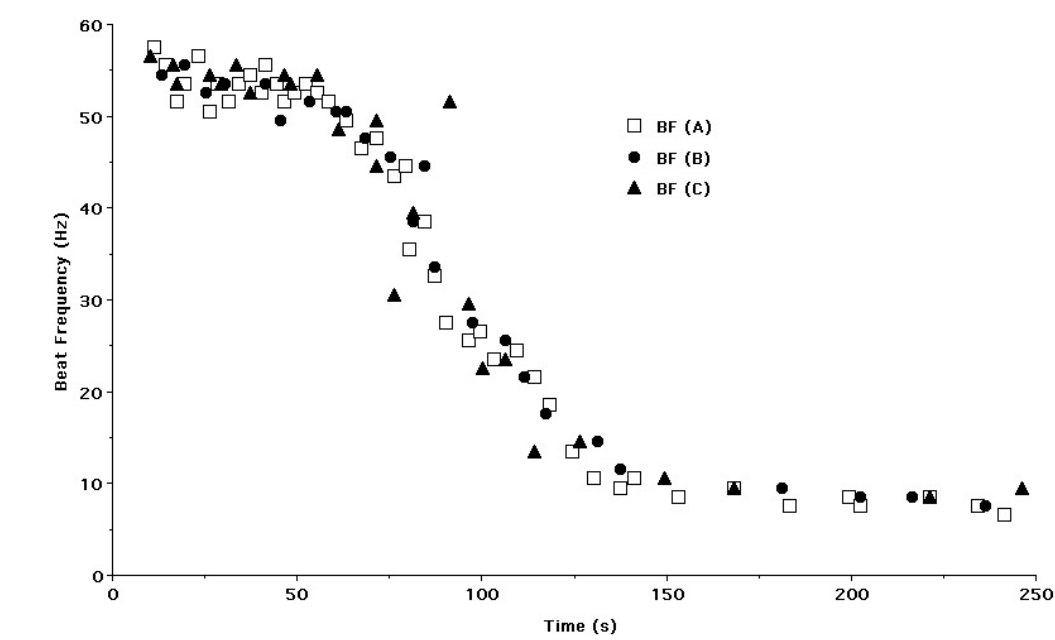


Figure 6

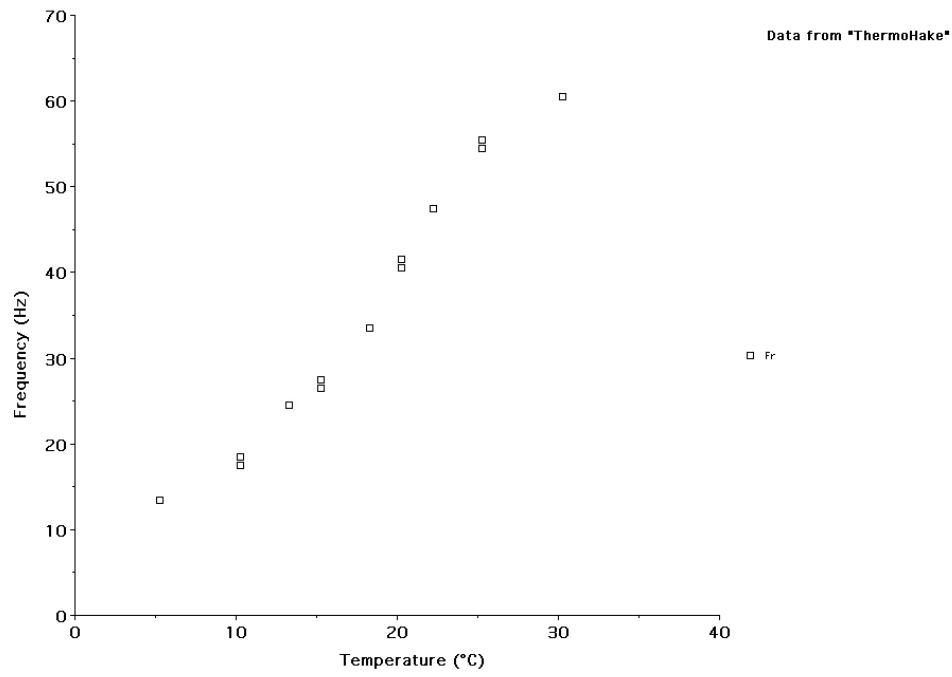


Figure 7a

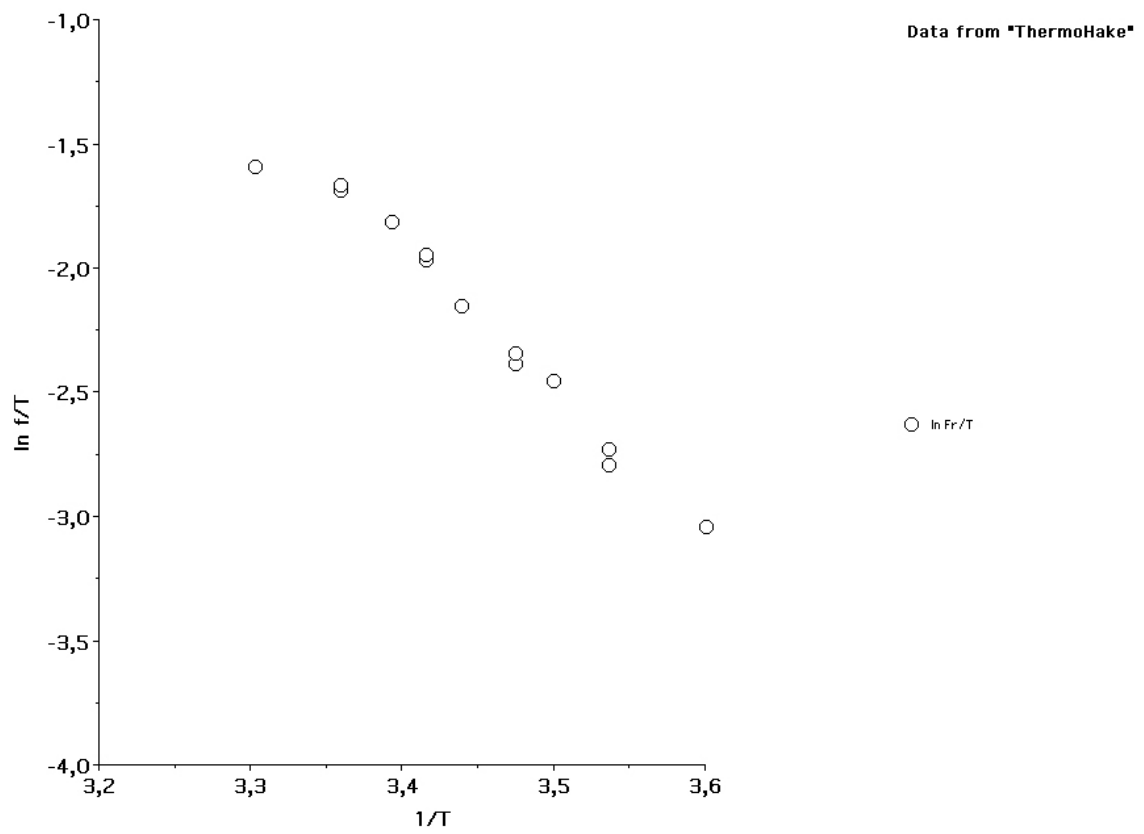


Figure 7b